Thermochimica Acta, 78 (1984) 113–122
Elsevier Science Publishers B.V., Amsterdam – Printed in The Netherlands

THERMAL DECOMPOSITION OF THE GRAPHITE OXIDATION PRODUCTS

A. MARTÍN RODRÍGUEZ

Departamento de Química Inorgánica, Facultad de Farmacia de Valencia, Valencia (Spain)

PEDRO VALERGA JIMÉNEZ

Departamento de Química Inorgánica, Facultad de Ciencias de Cádiz, Cádiz (Spain)

(Received 8 February 1984)

ABSTRACT

The graphite oxidation products were obtained by cold oxidation at 0 °C of graphite in liquid medium. They were dehydrated over P_2O_5 and characterized by chemical analysis and X-ray diffraction. Their thermal decomposition was studied by thermogravimetry (TG), differential thermal analysis (DTA), and gas chromatography (GC). The powder diagrams of the samples obtained by heating at 270 °C were recorded. The residues which were obtained from strongly oxidized products showed a new reflection (spacing between 4.3 and 4.5 Å).

INTRODUCTION

The graphitic oxides can be obtained by the oxidation of graphite in liquid medium, using either the Staudenmaier [1] or Hummers–Offeman method [2]. The product is a laminar and non-stoichiometric solid with a great trend to intercalate polar substances since it holds oxygenated groups inserted in its layers. Graphite oxide (GO) is a thermolabile compound. When it is subjected to rapid heating it deflagrates spectacularly [3,4]. The thermal decomposition at 120,150 and 190 °C of a graphite oxide, previously dried, has been studied by de Boer and van Doorn [5], who observed a dependence between the composition of the evolved gases and the heating rate.

There is a temperature of flash decomposition when the deflagration occurs. This temperature was used by Nazarov and co-workers in the characterization of the graphitic oxides; 170 °C [6] for a graphite oxide obtained by the Hummers–Offeman method; and 210 °C [7] for another one obtained in anhydrous nitric acid. Nevertheless, there is no literature on the thermal decomposition of graphite oxidation products partly oxidized in relation with the progress of the graphite attack.

0040-6031/84/$03.00

Along with other chemical type techniques, the oxidation kinetics of graphite in liquid medium has a considerable importance in the study of the graphitization process [8]. Those chemical techniques are complementary to physical techniques as X-ray diffraction or electron microscopy. In this work the thermal decomposition of graphite oxides and other products of the graphite partial oxidation are studied.

EXPERIMENTAL

Two different kinds of graphite samples are used. Both samples were polycrystalline graphites, one natural (N-graphite) from Degussa (Germany) and another one synthetic (A-graphite), artificially prepared by Sigri-Elektrographite GmbH (Germany). The graphites were ultrapure materials and they exhibit very similar powder diagrams. The oxidation products were prepared from these graphites with a particle size between 44 and 60 μm. Staudenmaier's method was chosen. Ground graphite in a beaker was subjected to attack by nitric and sulfuric acids at 0 °C. A few portions of $KClO_3$ were added to the beaker during the reaction. The oxidation attack was interrupted at 6, 12, 24, 32, 40, 48, 56, 64, 72, 84, 96, 108 and 120 h by dilution with 10 l of distilled water at 0 °C. The samples were washed with diluted HNO_3 and distilled water, and dried in a stove at 40 °C.

The oxidation products (40–60-μm particle size) were kept in a dessicator over sulfuric acid (density = 1.24 g cm^{-3}, water pressure = 12.7 Torr at 20 °C) until a constant weight was maintained, and later in a dessicator with P_2O_5 under vacuum, where some water was lost, until a constant weight was regained.

The chemical analysis was carried out by means of a Herrmann–Moritz analyzer (model EH-64). An oxygen flux at 25 cm^3 min^{-1} (purity = 99.998%) was used, through all operations performed, it was ensured that the samples did not deflagrate, therefore, the non-oxidized graphite was thoroughly burnt.

The powder diagrams were recorded by means of a Siemens' set (model D-500) using Cu *K* radiation, an Agfa–Gevaert film Structurix (Model-NDT) system, and a 114.9 mm diameter camera (Philips PW 1024/30). The debyegrams were transformed and plotted by a KD-540 microphotometer.

The thermal analysis (TG and DTA) was carried out by means of an analyzer system (Mettler TA-HE 20). The rates of heating were 6 °C min^{-1} to 140 °C, then 1 °C min^{-1} so that the samples did not deflagrate. The thermal decomposition under inert atmosphere was performed using a helium flux at a rate of 60 cm^3 min^{-1}. The gases evolved were analyzed by means of a Hewlett–Packard chromatograph.

Further information about the thermal decomposition of samples N-120 and A-120 was obtained in a simple TPD–MS device, previously described [9], operating in a flow of helium at normal pressure.

RESULTS AND DISCUSSION

Characterization

From the chemical analysis it was observed that the C/O ratio tends to a value of 2.0 in the samples with a longer oxidation time. This is the minimum ratio value for graphitic oxides obtained in a similar way. Nevertheless, it was also observed that the strongly oxidized samples from artificial graphite held more oxygen than similar samples from natural graphite. This could be explained by a larger amount of carbonyl, epoxy and peroxide groups in the samples obtained from N-graphite oxidation. Likewise, we must consider a greater content of carboxyl groups, which are linked to the edges of the layers [3,10]. On the other hand, in the samples from N-graphite with a shorter oxidation time (between 6 and 40 h), the C/O ratio is smaller than in the samples from A-graphite. This is due to the different crystalline perfection in N-graphite and A-graphite, evidenced by a different reactivity against the oxidizing reagents. Thus, the graphite originating from the graphitization of the binder is more easily attacked than the rest, so that a disintegration into smaller particles or polycrystals appears. The behaviour of both graphites is different in the beginning due to the bigger crystalline dimensions and the better layer perfection in natural graphite. Later, the behaviour becomes very similar, this fact is caused by the disintegration, and the graphite oxides obtained are very similar compounds.

We used the Hull–Davey chart for a rapid and qualitative study [11] of the debyegrams. A progressive disappearance of the (002) reflection corresponding to graphite and a simultaneous appearance of a reflection corresponding to graphitic oxide were observed in the powder diagrams (Fig. 1). An intensity decrease in the (101) reflection and the disappearance of the (100) reflection were also observed in samples with an intermediate oxidation time. In the samples that were oxidized more than the intermediate products the intensity of the band in the site of the old (100) band increased again, now showing a remarkably asymmetric shape. In the samples with $\geqslant 56$ h oxidation, the (002) reflection corresponding to the graphite was not observed. In the oxidation products with 24–48 h oxidation (natural series) or 24–48 h (artificial series) the (002) reflection corresponding to the grapnite and the graphitic oxide band appeared simultaneously. Two shorter bands appeared in the sites of the old (100) and (110) reflections. These reflections relate to the distances between planes parallel to the *c*-axis, which did not change much during the process. Nevertheless, the *c*-parameter increased as a result of the cleavage imposed by the functional group insertion in the layers. A strong decrease in the crystalline arrangement of the samples with reaction times from 24 to 48 h was indicated by the lower intensity of the bands in the sites corresponding to the (100) and (101) reflections of graphite. In the following stages of the oxidation process the

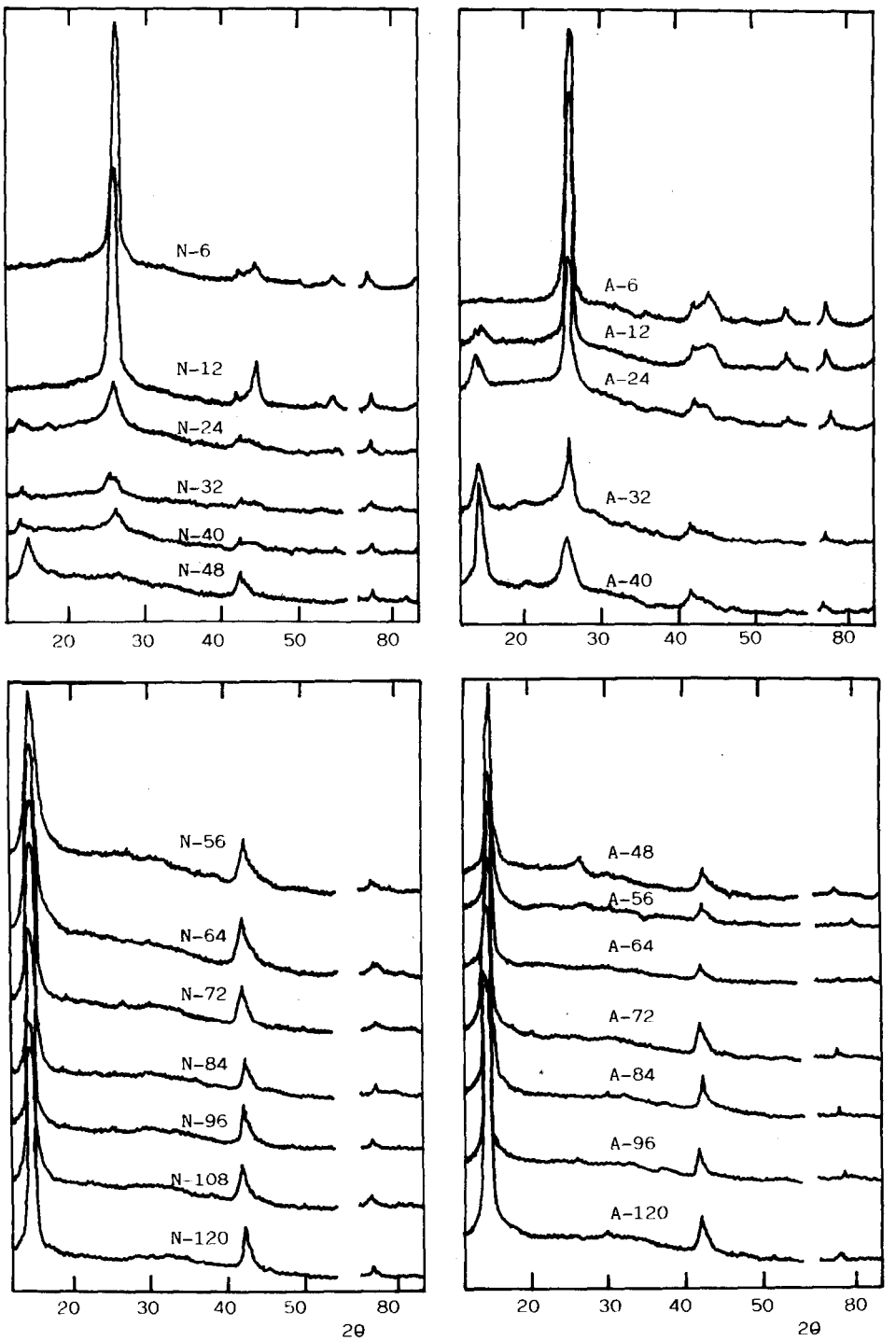

Fig. 1. Powder diagrams of the graphite oxidation products.

intensity of the former increased, whereas the latter did not appear. It could have been included in the former band, since it must be near to the first reflection due to the *c*-parameter increase.

From the chemical analysis and the X-ray diffraction diagrams, the samples oxidized during $\geqslant 72$ h can be considered as graphitic oxides. The remaining are intermediate oxidation products, composed of graphite and graphitic oxide which are probably linked in each layer.

Thermal decomposition

When the graphitic oxides and other strongly oxidized products were subjected to a heating rate of 6 °C min^{-1} they showed a thermolabile behaviour. These samples, in particular the products originated from A-graphite (Fig. 2), deflagrated spectacularly at 230 °C (A-48 and the following more oxidized samples). Nevertheless, it is possible to hinder the deflagration with a very slow heating rate (1 °C min^{-1}). In this way, the cold oxidation compounds exhibit three stages in their thermal decomposition.

In the first stage an endothermic effect, due to dehydration, occurs. The temperatures for which a maximum peak appears are summarized in Table 1. The weight loss is similar to that of each sample when moved from a desiccator over H_2SO_4 to one over P_2O_5. The gas chromatography indicated that the water is the main gas evolved (Fig. 3).

In a second stage (200–240 °C) the thermal decomposition of graphitic oxide occurs. In this case CO_2 and CO evolve in addition to water (Fig. 3). The DTA peak shows an exothermic effect. The temperatures at the maximum are summarized in Table 2, together with the weight loss for each sample. This stage (internal combustion or proper decomposition) is not

TABLE 1

The first stage of thermal decomposition: the weight loss and the temperature at the maximum in DTA

Sample	ΔW (%)	T (°C)	Sample	W (%)	T (°C)
N-12	0.0	–	A-12	–	–
N-24	2.0	50	A-24	9.0	67
N-32	1.5	50	A-32	3.0	–
N-40	5.0	75	A-40	8.0	70
N-48	4.0	75	A-48	12.0	70
N-56	10.0	70	A-56	14.5	70
N-64	15.5	85	A-64	15.0	75
N-72	14.0	70	A-72	17.0	80
N-84	15.5	85	A-84	16.0	80
N-96	15.5	80	A-96	17.0	75
N-108	15.0	80	A-108	–	–
N-120	17.0	80	N-120	17.0	80

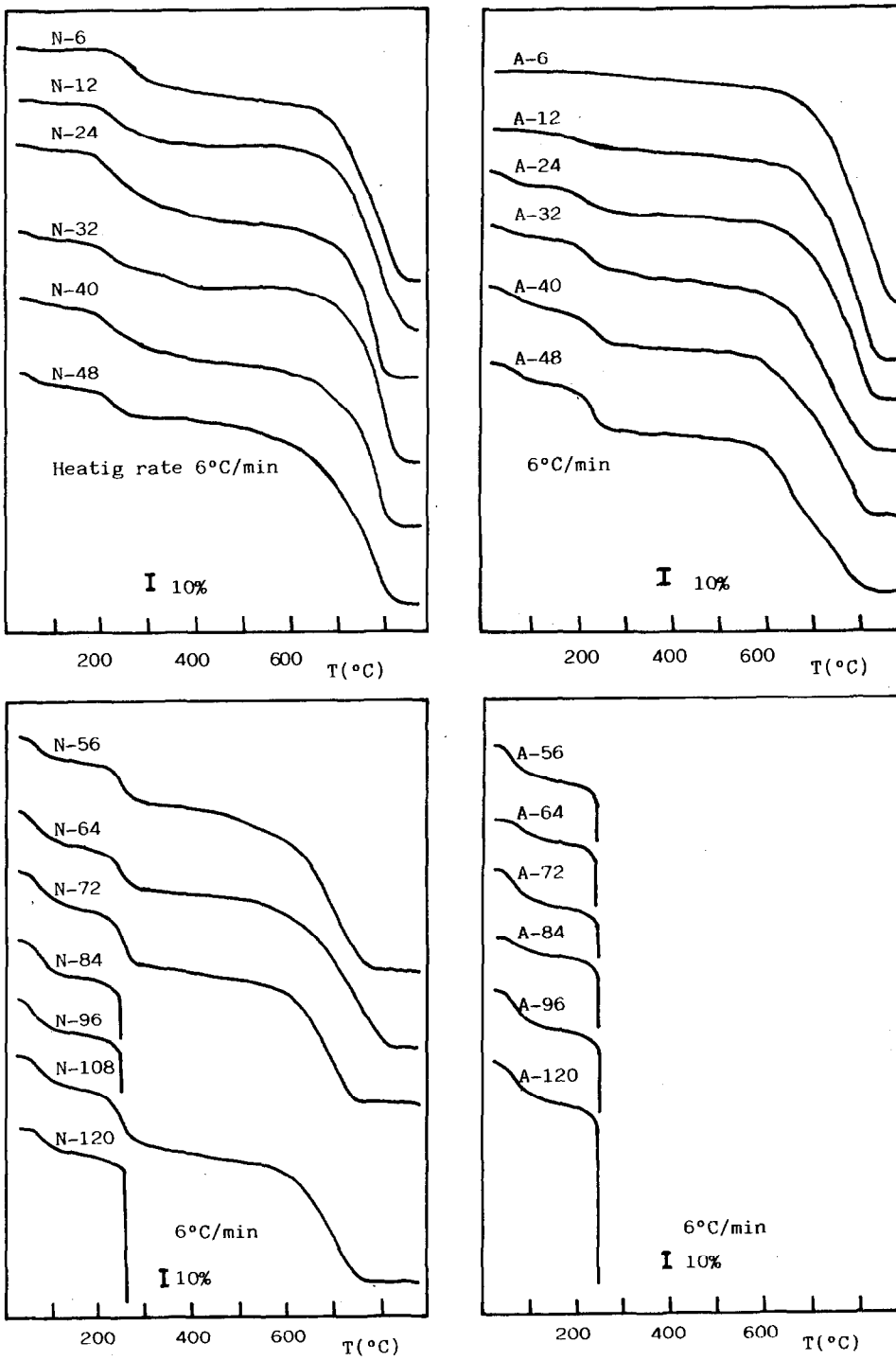

Fig. 2. Thermal decomposition of the graphite oxidation products.

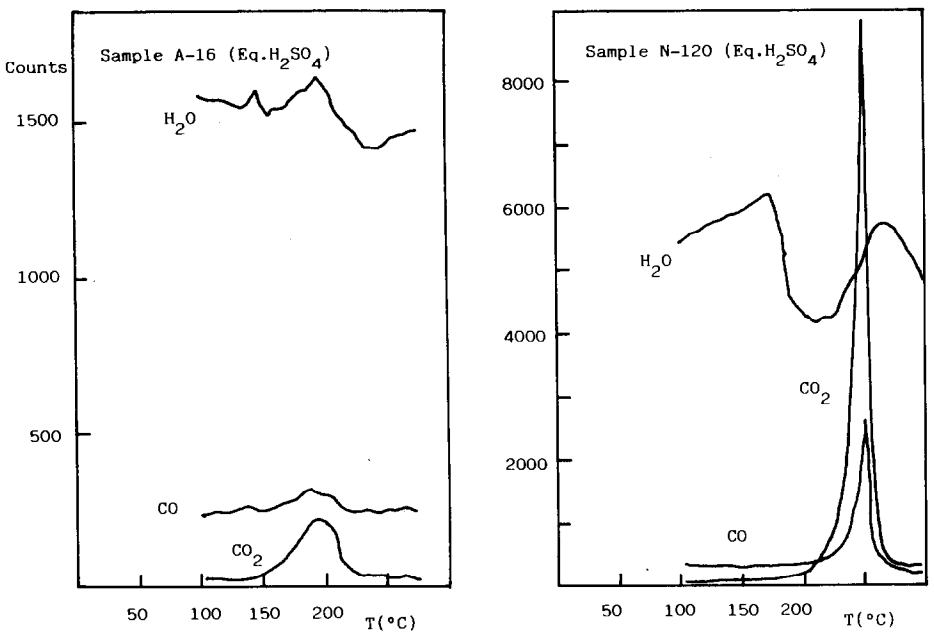

Fig. 3. Thermal decomposition: gases evolved during the first and second stages of decomposition.

finished at 270 °C, when a portion of the decomposition product was taken.

The third stage is a combustion which does not occur under inert atmosphere (Fig. 4). The combustion of the carbonaceous residue in the air begins at variable temperatures (ranging from 540 to 700 °C) which are

TABLE 2

The second stage of thermal decomposition: the weight loss and the temperature at the maximun in DTA

Sample	ΔW (%)	T (°C)	Sample	W (%)	T (°C)
N-12	18.5	–	A-12	7.0	195
N-24	20.0	225	A-24	15.0	195
N-32	13.5	210	A-32	17.5	200
N-40	17.0	200	A-40	13.0	205
N-48	16.0	220	A-48	15.0	220
N-56	16.5	227	A-56	23.5	223
N-64	22.0	225	A-64	23.0	227
N-72	27.5	222	A-72	26.5	230
N-84	26.5	240	A-84	28.0	230
N-96	31.0	225	A-96	26.0	235
N-108	26.0	225	A-108	–	–
N-120	25.0	230	N-120	26.0	235

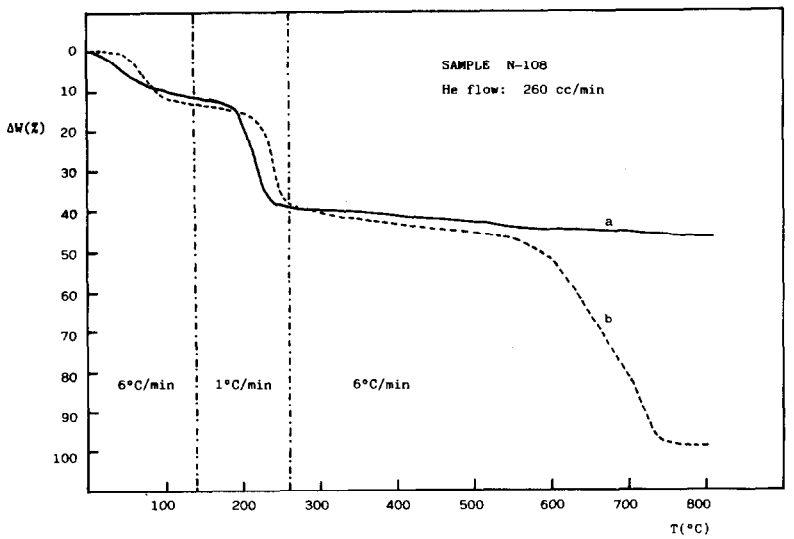

Fig. 4. Thermal decomposition: (a) under inert atmosphere; (b) in the air.

higher in the most oxidized compounds which indicates tautness in the layers of the intermediate oxidation products. In the air, the ashes at 800 °C are always smaller than 1% of the initial weight.

Samples N-120 and A-120 were analyzed by means of a DTP–MS device. Figure 5 shows H_2O and CO_2 evolutions with temperature. The loss of water is in good agreement with the amounts of water retained by the samples under a controlled atmosphere (H_2SO_4 $d = 1.24$ g cm^{-3}). N-120 lost 16% by thermal decomposition and retained 19% under controlled atmosphere.

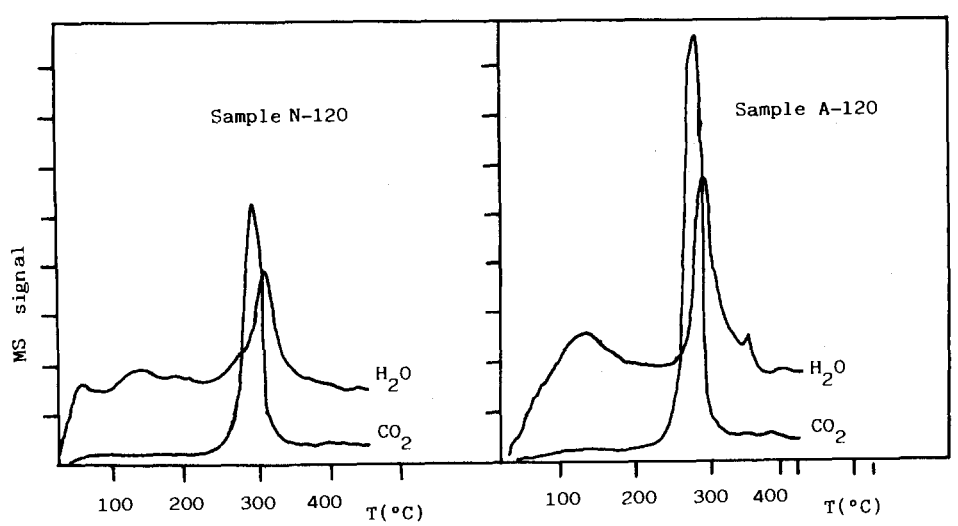

Fig. 5. DTP–MS traces of samples N-120 and A-120.

A-120 lost 18% by thermal decomposition and retained 20% under controlled atmosphere. Dehydration was not complete in the first stage of thermal decomposition due to a slow diffusion of water between the layers.

The powder diagrams of the samples obtained at 270 °C were recorded (Fig. 6). In these diagrams it is evident that the most intense band of graphitic oxide has disappeared (cf. Fig. 1). The decomposition products show diagrams where the (100) and (110) lines corresponding to graphite are kept. The (002) line of graphite also remains in the diagrams of the samples subjected to the smallest oxidation times, but is much more broad. This broadening increases in the strongly oxidized products, finally disappearing. Those samples which do not show the (002) line of graphite, show another one at 0.5 Å above the basal spacing of graphite. A new reflection also appears. The corresponding interlayer distance can vary between 4.3 and 4.5 Å, and it is more intense in the most strongly oxidized compounds.

The powder diagrams of the samples obtained at 270 °C showed that the

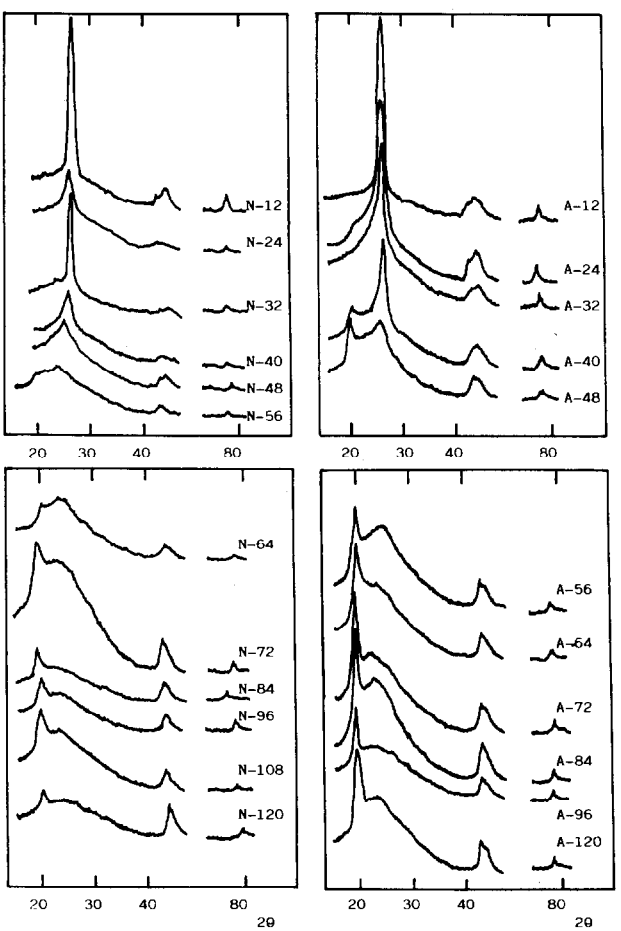

Fig. 6. Powder diagrams of the residues obtained by thermal decomposition at 270 °C.

carbonaceous layers were not completely broken by the internal combustion. In the products with a shorter oxidation time there was a very disordered carbonaceous residue which was getting more and more abundant when the oxidation time increased. The decomposition products still kept the lamellar arrangement, but their spacing was larger than the basal spacing in the graphite. The new reflection (4.3–4.5 Å) indicated that the thermal decomposition at 270 °C yields a new layered material which was also turbostratic.

CONCLUSIONS

The C/O ratio (in both natural and artificial series) decreased, attaining the value 2.0 after 64 h oxidation time. The powder diagrams showed a lamellar arrangement in every oxidation product obtained. The intermediate oxidation products were the most disordered samples. These compounds contained both graphite and graphitic oxide probably linked in each layer.

Some of the most oxidized products were thermolabile, they deflagrated at 230 °C when subjected to a 6 °C min^{-1} heating rate. This was avoided by using a very slow heating rate. Thus, the decomposition proceeded in three stages. In a first endothermic stage (at 80 °C) H_2O was evolved. In the second stage (200–240 °C) H_2O, CO_2 and CO were evolved, showing an exothermic effect. This stage was the internal combustion of graphitic oxide. Finally, the third stage (up to 530 °C) was the combustion of the carbonaceous residue which did not occur under inert atmosphere.

There is an intermediate stage in the cold oxidation of graphite. The compounds obtained in this stage did not deflagrate, but their temperatures of thermal decomposition are lower than the temperatures of graphitic oxide decomposition when the heating rate was very slow. These samples were disordered and tautness was very strong in their layers.

REFERENCES

1 L. Staudenmaier, Chem. Ber., 31 (1898) 1481.
2 W.S. Hummers, Jr. and R.E. Offeman, J. Am. Chem. Soc., 80 (1958) 1339.
3 U. Hofmann, A. Frenzel and E. Csalán, Justus Liebigs Ann. Chem., 510 (1934) 1.
4 R.C. Croft, Q. Rev. Chem. Soc., 14 (1960) 1.
5 J.H. de Boer and A.B.C. van Doorn, K. Ned. Akad. Wet., Versl. Gewone Verdag. Afd. Natuurkd., 61 (1958) 17.
6 A.V. Nikolaev, A.S. Nazarov and V.V. Lisitsa, Russ. J. Inorg. Chem., 19 (1974) 1862.
7 I.I. Yakolev, A.S. Nazarov and V.V. Lisitsa, Russ. J. Inorg. Chem., 22 (1977) 829.
8 M. Oberlin and J. Méring, Carbon, 1 (1964) 471.
9 S. Bernal, R. García and J.M. Rodríguez-Izquierdo, Thermochim. Acta, 70 (1983) 249.
10 J. de D. López González, A. Martín Rodríguez and J. Rodríguez Herrera, An. Quím., Ser. B, 76 (1980) 59.
11 A.W. Hull and W.P. Davey, Phys. Rev., 17 (1921) 549. In B.E. Warren (Ed.), X-Ray Diffraction, Addison-Wesley, London, 1969, p. 73.